Catal Lett (2009) 129:400–403
DOI 10.1007/s10562-009-9846-9

Selective Dissociation of O_3 and Adsorption of CO on Various Au Single Crystal Surfaces

I. Nakamura · A. Takahashi · T. Fujitani

Received: 4 January 2009 / Accepted: 5 January 2009 / Published online: 30 January 2009

Abstract The O_3 dissociation and CO adsorption on various gold single crystal surfaces were investigated using X-ray photoelectron spectroscopy, temperature-programmed desorption, and polarization modulation infrared reflection absorption spectroscopy (PM-IRAS). Dissociation of O_3 proceeded on the Au(111) surface at 323 K, whereas no O_3 dissociation occurs on the Au(100) surface, indicating that the O_3 dissociation on gold strongly depends on the structure of the gold surface. PM-IRA peaks of CO adsorbed on Au(111) and Au(100) were observed around 2,080 cm^{-1} at CO pressures above 0.5 Torr at 273 K. On the other hand, the peak of CO adsorbed on step sites was observed at 2,117 cm^{-1} above 0.01 Torr for Au(311). Thus, CO adsorbed preferentially onto the step sites of the gold surface.

Keywords Gold single crystal · O_3 Dissociation · CO Adsorption · Step sites · Structure sensitivity

1 Introduction

Gold nanoparticles supported on TiO_2 exhibit high catalytic activity for CO oxidation [1], and numerous investigations have been carried out to elucidate the source of this enhanced activity. Previous reports have identified quantum size effects that depend on the thickness of the gold nanoparticles [2, 3] and the presence of low-coordinated gold atoms on the surface of the nanoparticles [4–6] as possible contributors to the enhanced catalytic activity. The formation of active sites by the interaction of gold nanoparticles with oxide supports has also been reported. In particular, charge transfer from an oxide support to gold nanoparticles is reported to form negatively charged gold particles [7, 8] and to form a reactive gold–oxide interface [1, 9, 10]. Thus, there is ongoing controversy over the mechanism underlying the high catalytic activity observed for TiO_2-supported gold nanoparticle catalysts.

In addition to the aforementioned studies, reactions of both O_2 and CO on gold surfaces have been investigated by means of surface science techniques. In O_2 studies, the influence of sample temperature and O_2 pressure on O_2 dissociation at gold surfaces has been examined, but no O_2 dissociation was observed at any of the studied temperatures or pressures [11, 12]. By comparison, atomic oxygen is produced by the dissociation of O_3 from the Au(111) surface at 300 K under ultrahigh vacuum (UHV) conditions [13]. In CO studies, CO chemisorption has been observed on the Au(110) [14] and Au(111) [15] surfaces under elevated CO pressure at 300 K. Recently, we found that O_3 dissociation and CO adsorption depend strongly on the gold surface structure. Here, we report the O_3 dissociation and CO adsorption properties on gold single crystals with various surface structures.

2 Experimental

X-ray photoelectron spectroscopy (XPS, VG ESCALAB 220-i), temperature-programmed desorption (TPD) and polarization modulation infrared reflection absorption spectroscopy (PM-IRAS, Mattson RS/2) experiments were

---

I. Nakamura · A. Takahashi · T. Fujitani (✉)
Research Institute for Innovation in Sustainable Chemistry,
National Institute of Advanced Industrial Science and
Technology (AIST), 16-1 Onogawa, Tsukuba,
Ibaraki 305-8569, Japan
e-mail: t-fujitani@aist.go.jp

carried out in a UHV apparatus described in detail elsewhere [16]. XPS spectra were measured with Mg Kα radiation. PM-IRAS spectra were recorded at a resolution of 4 cm^{-1} with 500 scans. TPD experiments were carried out at a heating rate of 1.0 K/s.

Au(111), (100), and (311) single-crystal discs (8 mm diameter, 1 mm thickness, 99.999% purity, Surface preparation laboratory) were cleaned by cycles of Ar^+ sputtering and annealing at 900 K under vacuum. The cleanliness of the sample surfaces was verified by XPS or Auger electron spectroscopy (OMICRON SPECTALEED).

Experiments with O_2 (99.999% purity, TAIYO NIPPON SANSO Corporation) and CO (99.999% purity, TAIYO NIPPON SANSO Corporation) were carried out at 10^{-7}–10 Torr and 10^{-3}–10 Torr, respectively, and at a sample temperature of 273–323 K. The O_3 used for dosing was prepared in our laboratory from O_2 (99.999% purity) gas by means of a commercial O_3 generator. The O_2 gas was passed at a rate of 500 cc/min to the O_3 generator, and the effluent gas from the generator contained a mixture of approximately 0.4% O_3 and 99.6% unreacted O_2. The gold surfaces were exposed to O_3 at 10^{-8}–10^{-7} Torr and 323 K.

3 Results and Discussion

3.1 O_3 Dissociation

XPS measurements confirmed that no dissociative adsorption of O_2 occurred on surfaces of Au(111), Au(100) and Au(311) at O_2 pressures up to 10 Torr at 323 K, and this result agrees with previously reported results [11, 12]. By comparison, atomic oxygen was observed on the gold surfaces upon exposure of the surfaces to O_3 at 323 K under UHV conditions. Figure 1 shows the O 1s XP spectra for gold single-crystal surfaces exposed to 0–1,500 L of O_3. The O 1s peak due to atomic oxygen was observed at 529.2 eV for the Au(111) surface exposed to 3 L of O_3. The peak area increased with increasing O_3 exposure and saturation occurred at 600 L, where the O 1s/Au $4f_{7/2}$ peak area ratio was 0.0525. We estimated the saturation coverage of atomic oxygen on Au(111) was about 1.1 ML from the peak area of the O_2 desorption for O/Au(111), which was consistent with the reported coverage (1.2 ML) [13]. The binding energy of the O 1s peak shifted from 529.2 to 529.5 eV with increasing atomic oxygen. Saliba et al. [13] reported that the adsorption of electronegative oxygen species increases the work function, resulting in electron kinetic energy. Thus, the peak shift of O 1s was due to the electron transfer from the Au substrate into an oxygen adlayer. However, no atomic oxygen was observed on the Au(100) surface even at an O_3 exposure level of 1,500 L. By comparison, adsorbed atomic oxygen was observed on the Au(100) surface by dosing atomic oxygen at 300 K [17]. Thus, we conclude that dissociation of O_3 does not proceed on the Au(100) surface. The adsorption energies of atomic oxygen on the (100) face of the Au(211) surface and on the (111) face of the Au(221) surface have been calculated to be 2.91 and 3.09 eV, respectively [18]. Furthermore, the activation energies for O_2 desorption from the O/Au(111) [13] and O/Au(110) [12] surfaces are 126 and 132 kJ/mol, respectively. These reported values indicate that the adsorption and desorption properties of adsorbed oxygen atoms are similar regardless of the gold surface structure. Thus, we hypothesize that the extent of O_3 dissociation on gold depends on the structure of the gold surface.

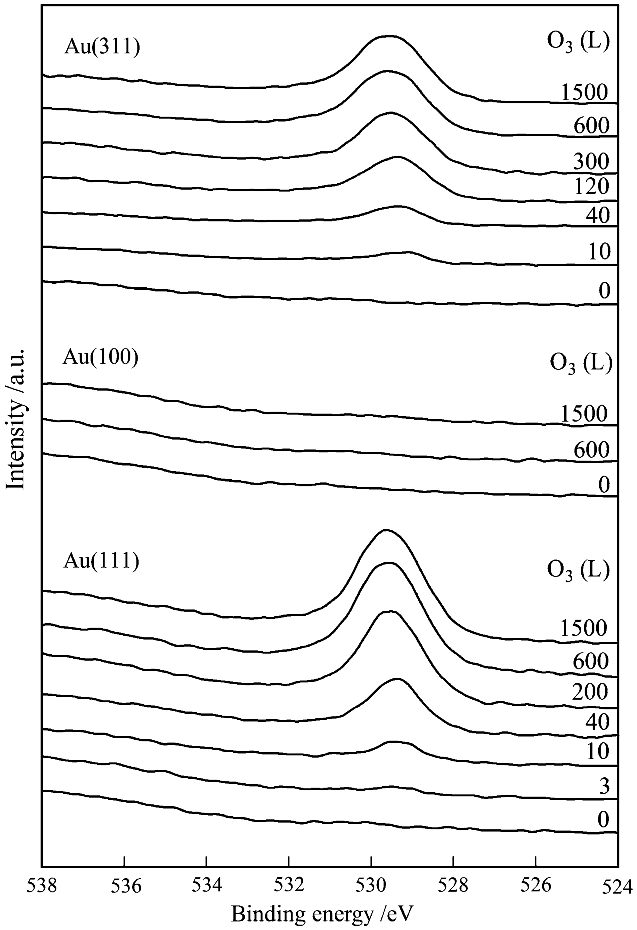

Fig. 1 O 1s XP spectra for the Au(111), (100), and (311) surfaces exposed to 0–1,500 L of O_3 at 323 K

The peak area of O 1s for the Au(311) surface was saturated at 600 L of O_3 exposure, which was the same exposure as Au(111), and the corresponding O 1s/Au $4f_{7/2}$ peak area ratio was 0.0296. The saturation coverage of atomic oxygen on the Au(311) surface was about half of that observed on the Au(111) surface. We also determined the initial formation rates of atomic oxygen at each gold crystal from the slopes of the transient portions of the curves for the O 1s/Au $4f_{7/2}$ ratio versus O_3 exposure time. The initial formation rate of atomic oxygen for the Au(311) surface was estimated to be half the rate determined for the Au(111) surface. The exposed (111) face on Au(311) was half of that on Au(111). These results clearly indicate that O_3 dissociation proceeds selectively over the (111) face of gold surfaces.

We also investigated the desorption properties of atomic oxygen adsorbed onto the gold surfaces. The TPD spectra of O_2 after exposure of the gold surfaces to various levels of O_3 are shown in Fig. 2. The O_2 desorption peak was observed at 560 K for the Au(111) surface exposed to 3 L of O_3. A second desorption peak appeared at 590 K after exposure to 40 L of O_3. At exposures above 120 L, the intensity and the temperature of the peak at 560 K increased with increasing O_3 exposure, whereas the peak intensity at 590 K remained constant. The adsorption energies of atomic oxygen on threefold hollow sites and bridge sites on the gold surfaces have been calculated to be 2.5–2.8 and 2.6–3.1 eV, respectively [18], indicating that the adsorption energy of atomic oxygen on gold surfaces does not vary substantially between adsorption sites. By comparison, the oxygen-containing Au(111) surface undergoes reconstruction to form a superstructure with a moiré-type pattern. This reconstruction arises from the periodic height modulation induced at the surface by a small lattice mismatch and a slight rotation between the topmost two gold layers [13, 19]. Therefore, we conclude that the two O_2 desorption peaks for the atomic-oxygen-saturated Au(111) surface reflect reconstruction of a part of the Au(111) surface during O_3 exposure rather than a difference in adsorption sites. As such, we assigned the peaks at lower and higher temperature to O_2 desorption from unreconstructed (111) sites and from reconstructed sites on the Au(111) surface, respectively. In contrast, Saliba et al. [13] observed only one desorption peak at 550 K for the atomic-oxygen-saturated Au(111) surface. This may be due to the difference in the heating rate used in TPD experiments.

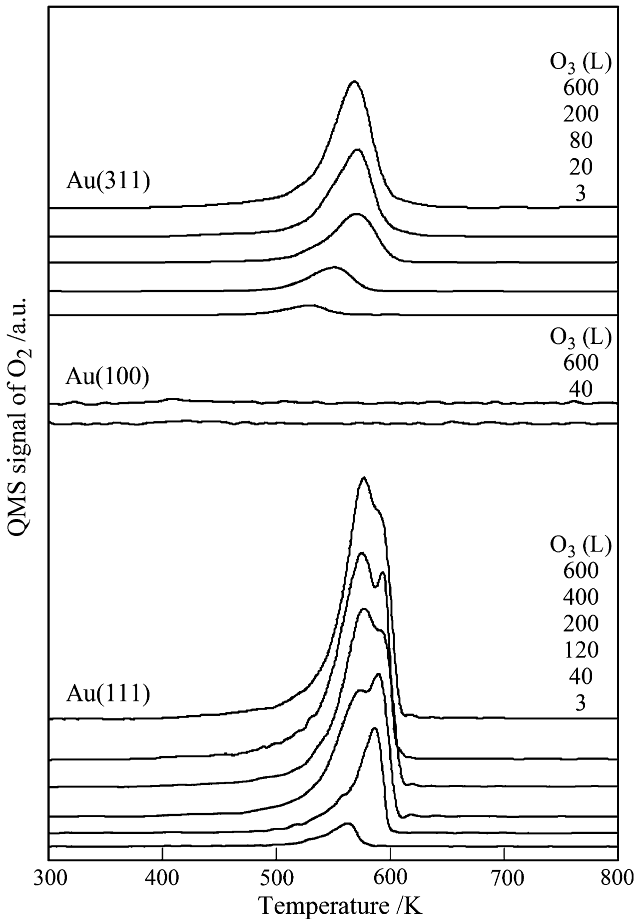

Fig. 2 TPD spectra of O_2 desorption following O_3 exposure of the Au surfaces

Only one desorption peak appeared in the TPD spectrum of the Au(311) surface (Fig. 2). The temperature of this peak is consistent with that observed for the desorption peak from unreconstructed (111) sites of the Au(111) surface. The narrow (111) face of the two-atom-row over Au(311) suggests that the reconstructed surface with a moiré-type pattern is not induced by oxygen adsorption. This result indicates that atomic oxygen adsorbed only onto the (111) face of the Au(311) surface and demonstrates that O_3 dissociation on the gold surface is structure-sensitive.

3.2 CO Adsorption

We found that the adsorption behavior of CO also depends on the gold surface structure. Figure 3 shows the PM-IRA spectra for the Au(111), (100), and (311) surfaces during CO exposure at various pressures at 273 K. No CO adsorption was observed for any of the gold surfaces at CO pressures below 0.01 Torr. At 0.5 Torr, CO adsorption peaks at 2,070–2,080 cm^{-1} were observed for Au(111) and Au(100); these peaks were assigned to the CO adsorbed on atop sites (atop-CO) [15, 20, 21]. The adsorption behavior of CO on Au(111) and Au(100) showed a similar dependence on the CO pressure: the peak intensities increased with increasing pressure up to 3 Torr and then remained constant for both surfaces at 5 and 10 Torr.

By comparison, the CO adsorption peak was observed at 2,117 cm^{-1} for Au(311) at 0.01 Torr, and the peak intensity increased with increasing CO pressure. At pressures above 0.5 Torr, the peak intensity decreased and a new adsorption peak appeared around 2,070 cm^{-1}. The intensity of this second peak increased with increasing CO pressure up to 5 Torr and then remained constant at 5 and 10 Torr. This adsorption behavior was similar to that observed for CO adsorbed onto the Au(111) and Au(100)

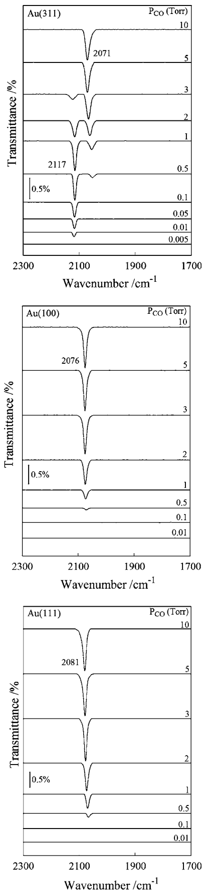

Fig. 3 PM-IRA spectra for the Au(111), (100), and (311) surfaces during CO exposure at various pressure (0.005–10 Torr) at 273 K

surfaces, indicating that the CO peak around 2,070 cm^{-1} was due to atop-CO adsorbed onto terrace sites of Au(311). The CO adsorption on the Au(322) surface has been investigated by IRAS [22]. The stretching mode of atop-CO adsorbed on step sites was observed at 2,124 cm^{-1}, on the other hand, the atop-CO peak on terraces sites was seen at 2,110 cm^{-1} by CO exposure at the condition of 92 K of sample temperature and below 1×10^{-5} mbar of CO pressure. It was thus demonstrated that the frequency of CO adsorbed on step sites over the gold surface is high compared with that on terrace sites. Therefore, we assigned the CO peak at 2,117 cm^{-1} to atop-CO adsorbed onto step sites of Au(311). Our findings demonstrated that the step sites on the gold surface are effective for CO adsorption under low CO pressure.

We demonstrated that CO adsorbs onto gold single crystal surfaces, whereas O_2 dissociation does not take place. We thus consider that the CO oxidation does not occur on the gold single crystal because no atomic oxygen was present on gold surface. By comparison, CO oxidation can proceed on the supported gold nanoparticle catalyst, considering that O_2 can dissociate on the supported gold surface. On the basis of these results the nature of the support for the gold nanoparticle catalyst may function to create the dissociation sites for O_2.

4 Conclusions

1. O_3 Dissociation over gold surface proceeded selectively on the (111) face.
2. CO Adsorbed preferentially onto the step sites of the gold surface.

Acknowledgment This work was supported by the Japan Science and Technology Agency, JST, CREST.

References

1. Haruta M (1997) Catal Today 36:153
2. Valden M, Lai X, Goodman DW (1998) Science 281:1647
3. Chen MS, Goodman DW (2004) Science 306:252
4. Lemire C, Meyer R, Shaikhutdinov SK, Freund HJ (2004) Surf Sci 552:27
5. Lopez N, Janssens TVW, Clausen BS, Xu Y, Mavrikakis M, Bligaard T, Nørskov JK (2004) J Catal 223:232
6. Remediakis IN, Lopez N, Nørskov JK (2005) Appl Catal A 291:13
7. Yoon B, Häkkinen H, Landman U, Wörz AS, Antonietti JM, Abbet S, Judai K, Heiz U (2005) Science 307:403
8. Chen M, Cai Y, Yan Z, Goodman DW (2006) J Am Chem Soc 128:6341
9. Schubert MM, Hackenberg S, van Veen AC, Muhler M, Plzak V, Behm RJ (2001) J Catal 197:113
10. Grunwaldt JD, Baiker A (1999) J Phys Chem B 103:1002
11. Canning NDS, Outka D, Madix RJ (1984) Surf Sci 141:240
12. Sault AG, Madix RJ, Campbell CT (1986) Surf Sci 169:347
13. Saliba N, Parker DH, Koel BE (1998) Surf Sci 410:270
14. Jugnet Y, Cadete Santos Aires FJ, Deranlot C, Piccolo L, Bertolini JC (2002) Surf Sci 521:L639
15. Piccolo L, Loffreda D, Cadete Santos Aires FJ, Deranlot C, Jugnet Y, Sautet P, Bertolini JC (2004) Surf Sci 566–568:995
16. Nakamura I, Hamada H, Fujitani T (2003) Surf Sci 544:45
17. Davis KA, Goodman DW (2000) J Phys Chem B 104:8557
18. Liu ZP, Hu P, Alavi A (2002) J Am Chem Soc 124:14770
19. Chevrier J, Huang L, Zeppenfeld P, Comsa G (1996) Surf Sci 355:1
20. Jong AM, Niemantsverdriet JW (1994) J Chem Phys 101:10126
21. Fujitani T, Nakamura I, Takahashi A, Haneda M, Hamada H (2008) J Catal 253:139
22. Ruggiero C, Hollins P (1996) J Chem Soc Faraday Trans 92:4829